Carbohydrate Polymers 112 (2014) 486–493

Contents lists available at ScienceDirect

Carbohydrate Polymers

journal homepage: www.elsevier.com/locate/carbpol

The role of poly-M and poly-GM sequences in the metal-mediated assembly of alginate gels

Matthew B. Stewart[a,b,*], Stephen R. Gray[a,b], Todor Vasiljevic[a,c], John D. Orbell[a,b]

[a] Institute for Sustainability and Innovation (ISI), Victoria University, PO Box 14428, Melbourne 8001, VIC, Australia
[b] College of Engineering and Science, Victoria University, PO Box 14428, Melbourne 8001, VIC, Australia
[c] College of Health and Biomedicine, Victoria University, PO Box 14428, Melbourne 8001, VIC, Australia

ARTICLE INFO

Article history:
Received 24 January 2014
Received in revised form 28 May 2014
Accepted 1 June 2014
Available online 11 June 2014

Keywords:
Alginate sequence
Sodium alginate
Alginate gels
Molecular dynamics
Calcium coordination

ABSTRACT

Whilst the involvement of poly-G sequences in the formation of metal-mediated alginate gels has been previously studied in some detail, investigations into the role of poly-M and poly-GM sequences has been relatively neglected. In this regard, the binding of sodium and calcium ions to poly-M and poly-GM decamers, and their influence on chain aggregation, has been modelled by conducting a series of molecular dynamics simulations. This work complements a previous analogous study carried out for the poly-G decamer, whereby up to three strands are systematically introduced into each simulation. As in the previous study, this method allows intrinsic binding modes and interchain structural motifs to be revealed, that are consistent with those observed in available AFM images of consolidated 3-D networks. It is apparent from these studies that different sequences have different structural implications for metal-mediated chain association.

1. Introduction

Alginates are naturally occurring linear polyuronic acids found in various species of brown algae and bacteria (Donati & Paoletti, 2009; Gorin & Spencer, 1966; Goven, Fyfe, & Jarman, 1981). The polymeric chains consist of arrangements of β-D-mannuronic acid (M) and, α-L-guluronic acid (G) monomers, bound *via* (1 → 4) glycosidic linkages. Experimental fractionation work has shown (Haug, Larsen, & Smidsrød, 1966; Haug, Larsen, & Smidsrød, 1967; Haug & Smidsrød, 1965) that alginates display a block copolymer structure of three distinct sequences. These blocks have been identified to be either polyguluronate (referred to herein as poly-G), polymannuronate (poly-M), or alternating GM sequences (poly-GM) (Haug et al., 1966), Fig. 1. High-resolution proton and carbon NMR (Grasdalen, 1983; Grasdalen, Larsen, & Smidsrød, 1977; Grasdalen, Larsen, & Smidsrød, 1979; Grasdalen, Larsen, & Smidsrød, 1981) as well as lyase degradation and mass spectrometry experiments (Holtan, Bruheim, & Skjåk-Bræk, 2006), have shown that, in alginates extracted from algae, the relative G:M ratios and copolymer block lengths of the three sequences, are conserved and species-specific. In contrast, alginates isolated from bacteria tend to show more variable composition within species, as well as a propensity to be randomly acetylated (Ertesvåg, Valla, & Skjåk-Bræk, 1996; Skjåk-Bræk, Grasdalen, & Larsen, 1986), which may be related to subtle differences in biological function between plants and bacteria.

In the presence of divalent cations (commonly Ca^{2+}), alginates display gelling and water retaining properties which make them useful for various applications across a number of industries including the food and water treatment industries and in medical/dental applications (BeMiller, 2009; Davis, Volesky, & Mucci, 2003; Donati & Paoletti, 2009; Langer & Tirrell, 2004). Such gelling is known to occur *via* metal-mediated interchain interactions that may be visualized by techniques such as atomic force microscopy. The areas where interchain interactions occur within these networks are commonly referred to as 'junction zones'.

Here, we have employed a molecular dynamics method that has been specifically developed (Stewart, Gray, Vasiljevic, & Orbell, 2014) to probe the *intrinsic* binding of sodium and calcium ions to poly-M and poly-GM decamers in an aqueous environment, with a view to discerning metal-mediated inter-strand motifs that could form the basis for the subsequent assembly of 3-D networks. In this regard, such structures, which are inherently of an intermediate nature, may provide structural insights into potential gel assembly mechanisms. Previous work under the same computational method has revealed unique junction zones and structural motifs

* Corresponding author. Tel.: +61 3 9919 7641; fax: +61 3 9919 8082.
E-mail addresses: Matthew.Stewart@vu.edu.au (M.B. Stewart), Stephen.Gray@vu.edu.au (S.R. Gray), Todor.Vasiljevic@vu.edu.au (T. Vasiljevic), John.Orbell@vu.edu.au (J.D. Orbell).

http://dx.doi.org/10.1016/j.carbpol.2014.06.001
0144-8617/

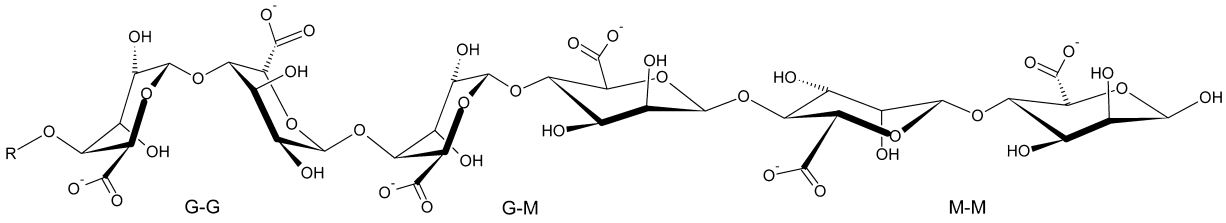

Fig. 1. A section of alginate polymer (deprotonated) showing the two different G and M monomers and the three different sequential units.

that are associated with the binding of Ca^{2+} to poly-G decamers (Stewart et al., 2014). This work was shown to be more informative in relation to possible 3-D network assembly than previous, more biased, simulations of the Ca^{2+}-mediated association of poly-G sequences (Braccini, Grasso, & Pérez, 1999; Braccini & Pérez, 2001; DeRamos, Irwin, Nauss, & Stout, 1997; Plazinski, 2011). The work presented here which, under the same computational method, focuses on the poly-M and poly-GM sequences, provides a more extensive overview of *in situ* alginate–ion interactions and helps to clarify the role that sequence, in particular, has to play in this process, especially with respect to the molecular details of interchain assembly.

2. Computational method

Simulations were carried out using a modified CHARMM all22 force field (MacKerell et al., 1998) and the NAMD 2.7 package (Phillips et al., 2005). Topology and parameter files for carbohydrates were edited to allow for the addition of the carboxylic acid groups. Atomic point charges were recalculated from density functional equilibrium geometry calculations, at the B3LYP/6-31G(d) level of theory, on the G and M monomers and reapplied to the topology. Oligomers of the two sequences (poly-M and alternating G-M), each 10 residues long and fully deprotonated, were constructed using the Visual Molecular Dynamics (VMD) program (Humphrey, Dalke, & Schulten, 1996) and optimised using MD in a TIP3P water box which measured 20 Å × 20 Å × 20 Å. These optimisations involved 2000 conjugate gradient minimization steps, followed by 2 ps of molecular dynamics simulation time under NVT conditions in a periodic box. The temperature and pressure was maintained using Langevin dynamics as implemented in NAMD. It must be noted that these initial optimisation simulations were not charge neutralised, as the effect of metal ions (including Na^+, which is the standard counter ion for alginates) was to be investigated. These optimised structures were used as starting geometries for the metal ion binding simulations.

The production simulations involved either one, two or (in the case of the Ca^{2+} ion environments only) three decamers. Where two decamer chains were present, the identical sequences were placed parallel, approximately 6 Å apart; where three chains were used, these were arranged parallel to each other, with their lateral cross-section forming a triangle. TIP3P water was then added, with 20 Å padding in all directions. Ca^{2+} ions were added randomly to the solvated system to neutralise the anionic charges of the oligomers. These ions were added *via* the Autoionize plugin in VMD with a minimum distance of 5 Å between the added ions and the solute or other ions. The ion placement was randomised so as to not potentially bias the simulation towards a particular outcome. Each system was again subjected to 2000 conjugate gradient minimisation steps, followed by a simulated annealing procedure. This has been introduced in order to overcome the inherent energy barriers in these simulations whilst keeping the simulation time as short as possible. Achieving this by traditional optimization methods requires the initial state of the system, in terms of the positioning of the Ca^{2+} ions, to reflect the expected outcome of the simulation—an approach that has been adopted in all previous MD studies on metal/alginate systems, *vide supra.* Since a major objective of this work is to avoid such bias, this simulated annealing protocol has been successfully implemented in order to readily identify more intrinsic outcomes. Notably, this approach has been validated in this study by the observed consolidation of well-behaved metal coordination geometries that are in good agreement with experimental data (Dudev & Lim, 2004; Einspahr & Bugg, 1981; Katz, Glusker, Beebe, & Bock, 1996). A major advantage of this method is that highly informative structural outcomes are obtained in a relatively short simulation time of less than 1 ns. This annealing procedure involved an initial increase in temperature to 650 K, with cooling of the system to 300 K in 50 K increments at 100 ps intervals, giving a final runtime of 0.8 ns. An NVT-ensemble and periodic boundary conditions were utilised for these annealing simulations with the temperature controlled *via* rescaling of all velocities every 2 ps. The equations of motion were integrated at 1 fs timesteps. Short-range nonbonded interactions were calculated at a 1 fs timestep with a van der Waals switching distance of 10 Å and overall nonbonded cutoff at 12 Å with long-range interactions integrated every 2 fs using the r-RESPA integrator. The Particle mesh Ewald (PME) method was used to describe the full-system periodic electrostatics. The short-range pairlist was updated every 10 fs for atoms within 14 Å. The simulation trajectory was written every 500 fs in order to provide good quality data with respect to interactions. All single chain simulation trajectories were analysed *via* calculation of the radial distribution functions for specific oxygen–metal ion interactions, utilising the g(r) GUI plugin of VMD (Humphrey et al., 1996).

3. Conventions

Structural conventions are described in Fig. 2. Simulations involving a single alginate decamer are denoted by either 1× poly-M or 1× poly-GM. Those involving two such chains are denoted by either 2× poly-M or 2× poly-GM and those involving three such chains are denoted by either 3× poly-M or 3× poly-GM.

4. Results and discussion

There have been a number of previous studies into metal-mediated alginate gelling where the rationale is almost exclusively focused on the poly-G sequence (Braccini & Pérez, 2001; Li, Fang, Vreeker, & Appelqvist, 2007; Plazinski, 2011). However, it is not inappropriate to suggest that the other sequences also have important roles to play. In this regard, whilst there has been some limited interest regarding the influence of the poly-GM sequence with respect to interactions with various ions (Donati et al., 2005), there is a relative paucity of such studies, especially with respect to poly-M sequences. The work presented here utilizes molecular dynamics simulations, with a view to providing insights into the interaction

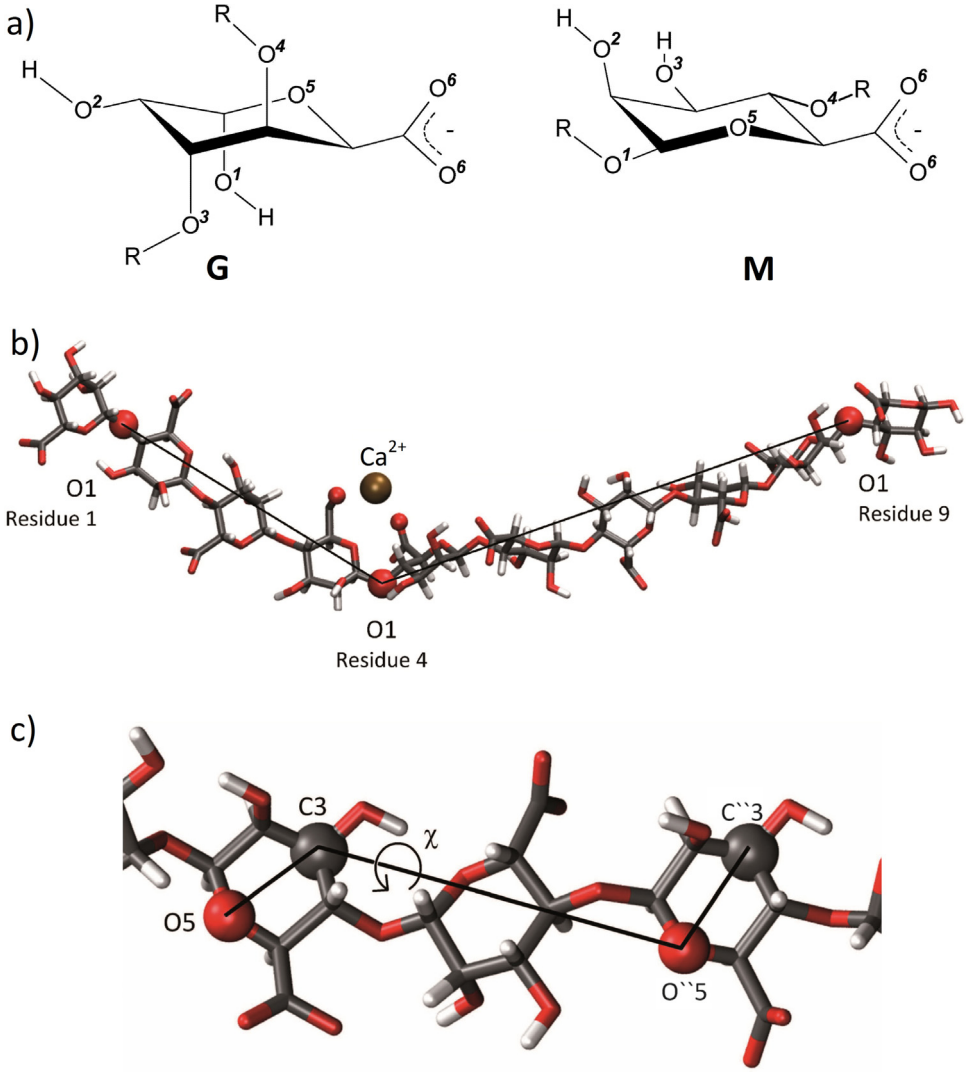

Fig. 2. (a) Alginate monomers showing the numbering scheme with respect to the oxygen atoms in (a) α-L-guluronate (G) and (b) β-D-mannuronate (M). *Notes*: (i) atoms referred to in the text that are in an adjacent monomer are marked with a dash. A double dash refers to atoms located two monomers away. An asterisk indicates that an atom is on a second chain. (ii) O6 refers to the oxygens of a delocalized carboxylate anion. (b) The convention used to measure the chain bend angle in the poly-M sequence. The O1 atoms (*i.e.* the oxygen atoms involved in the glycosidic linkage—red spheres) are used in this convention as these atoms are less likely to be affected by residue rotation during simulation and, therefore, provide a 'stable backbone'. The terminal O1 atoms involved in a glycosidic bond (here, those on residue 1 and residue 9) were therefore used in this measurement, with the vertex being at the site of the intrachain carboxylate bridge (here, at the O1 atom associated with residue 4). (c) The convention used to measure the twist of an alternating poly-GM sequence (χ). Here, two mannuronate residues are used to define the dihedral angle formed by O5-C3-O″5-C″3 (oxygen atoms—red spheres). Therefore, each dihedral angle involves residues of the same type only. (For interpretation of the references to colour in this figure legend, the reader is referred to the web version of this article.)

of Na^+ and Ca^{2+} ions with poly-M and poly-GM sequences, and to identify potential intrinsic binding modes that may contribute to the assembly of 3-D gels.

All simulations carried out in this work, irrespective of sequence identity, result in complexation with both Na^+ and Ca^{2+} ions. These oligomer–metal ion interactions are generally formed rapidly, with Ca^{2+} interactions observed to consolidate sooner within the simulations than Na^+. Notably, as with previous poly-G simulations (Stewart et al., 2014), chains agglomerated *only* when Ca^{2+} ions were involved—which is also consistent with experimental observations regarding the solubility of alginates in the presence of monovalent cations and hydrogel formation in the presence of divalent or multivalent cations (Donati & Paoletti, 2009). The detailed interactions of Ca^{2+} and Na^+ with the different oligomers and the configurations of the multichain systems are described below.

4.1. 1× Poly-M

When a single poly-M chain is simulated in an aqueous environment in the presence of Ca^{2+} ions, two Ca^{2+} binding modes are observed. The ion–alginate interactions are predominantly due to the Ca^{2+} ions binding directly to the negatively charged carboxylate groups. Indeed, the most common interaction is simply a carboxylate–Ca^{2+} ion interaction, which appears to have minimal effect on the chain conformation. However, a more disruptive interaction involves a Ca^{2+} ion coordinated by two carboxylate moieties on neighbouring residues of the same chain, Fig. 3a, *i.e.* an intrachain carboxylate–Ca^{2+}–carboxylate bridge. Usually, alginates have neighbouring carboxylate groups on opposite sides of the chain (*trans*); as might be expected in order to provide the maximum available distance between the anionic carboxylate moieties. This simulation displays evidence for the local stabilisation, *via*

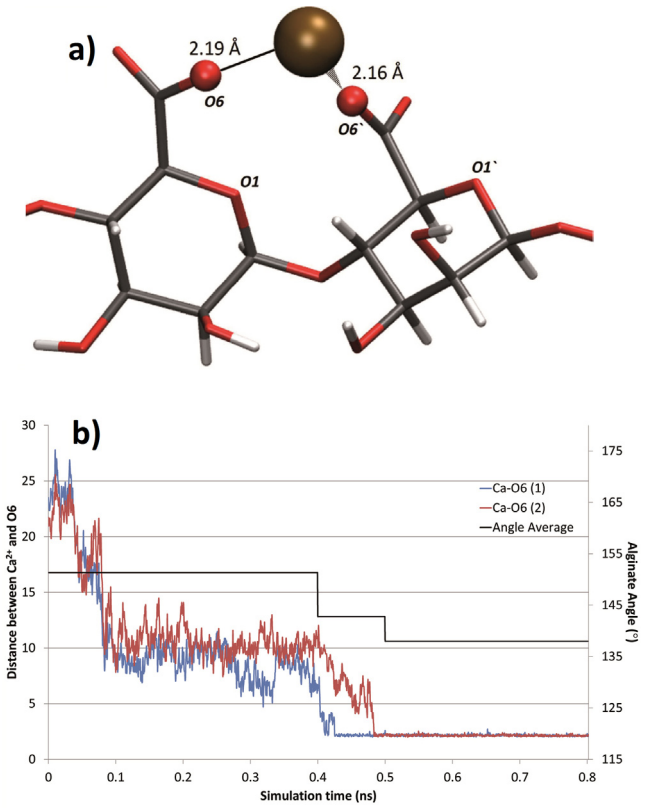

Fig. 3. (a) A close-up rendering of the intrachain carboxylate–Ca^{2+}–carboxylate bridge that was identified in the 1× poly-M simulation. The Ca^{2+} ion (brown sphere) is closely bound to the carboxylate groups (red spheres indicating interacting atoms) of neighbouring residues, due to a 180° rotation of the chain about the glycosidic bond between these two residues. Water molecules have been omitted for clarity. (b) Plot showing the bending angle, see Fig. 2b, of the poly-M chain in the presence of Ca^{2+} as well as the Ca^{2+}–carboxylic oxygen distances. As can be seen from this figure, the two concomitant carboxylate groups of the poly-M chain interact with the Ca^{2+} ion stepwise in a non-concerted mechanism. This process results in the bending angle of the chain reducing from 151.3° to 138.2°. This change in angle from the solvated chain suggests that the alginate in this case is not in its lowest energy geometry. This state appears to be stabilized by the ions. (For interpretation of the references to colour in this figure legend, the reader is referred to the web version of this article.)

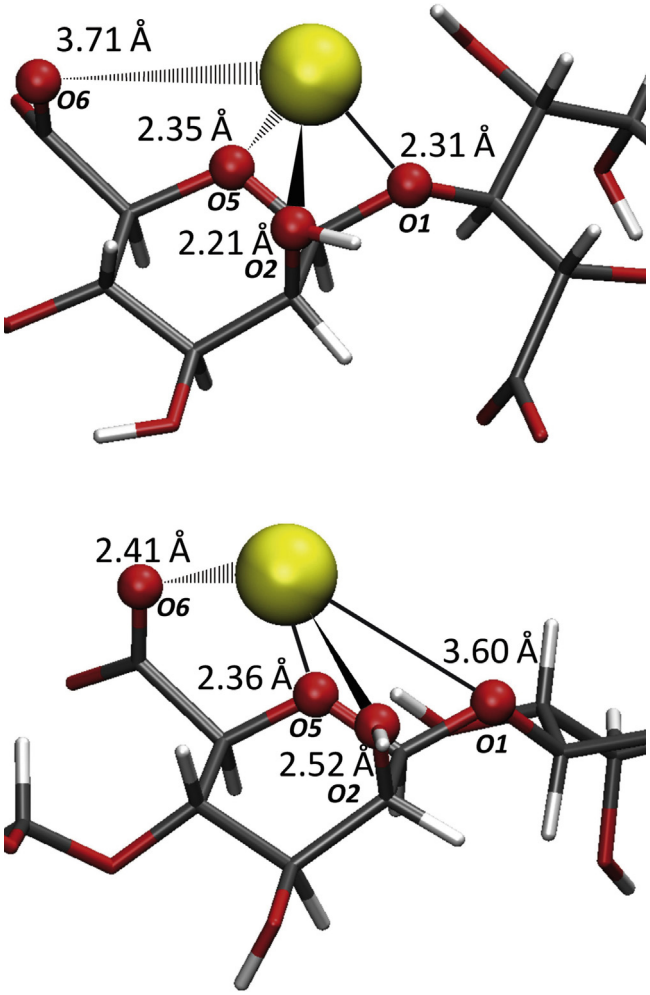

Fig. 4. A molecular dynamics snapshot of the proposed Na^+ poly-M binding site, in the two different modes that were identified, with the Na^+ ion (yellow sphere) interacting directly with the oxygens (red spheres). Water molecules have been omitted for clarity. (For interpretation of the references to colour in this figure legend, the reader is referred to the web version of this article.)

coordination of a Ca^{2+} ion, of the *cis* configuration. This binding mode is found to stabilise a bend in the poly-M chain which may be significant with respect to understanding alginate behaviour in solution and gel structural features. The bending angle, as defined in Fig. 2b, ranges from an average of 151.3° before coordination to 138.2°, after both carboxyl oxygen atoms have consolidated, Fig. 3b.

With Na^+ as the counter ion, a significantly different binding mechanism is evident from the simulation. The carboxylate moiety is not favoured in this simulation. Rather, the O1 atom appears to be the focus of a preferred binding site. The radial distribution function, Fig. S1, for this interaction suggests a preference for an 'egg-box'-type interaction. However, upon closer inspection it appears that there are two slightly different binding modes that flip from one to the other with relative ease, Fig. 4. Whilst there was some evidence (not shown) that this interaction stabilised a flat, rigid conformation of the poly-M chain, the interaction was very short lived. Therefore, any influence over chain conformation that this interaction modality might confer would be brief.

This appears to be the first identification of this particular type of interaction since it was first postulated in the original 'egg-box' paper by Grant, Morris, Rees, Smith, and Thom (1973). DeRamos et al. (1997) identified a slightly different possible binding mode; however, their model implicates the involvement of the O3 atom, instead of the O2 atom as we present here. Whether Ca^{2+} ions can also reside in this 'flattened' binding site was not immediately evident from our work. However, it is possible that this system, with further simulation time at a lower temperature, may relax into this structure. It is also possible that these types of interactions may be more prevalent at a higher concentration of Ca^{2+}, as previous studies have shown that poly-M sequences crystalize with Ca^{2+}, albeit at a significantly higher concentration than observed for poly-G sequences (DeRamos et al., 1997).

4.2. 2× Poly-M

A similar pattern of interactions is observed when a second chain is simulated in the presence of Na^+ ions, showing an approximately equivalent affinity of the sodium ions for O1 and O2, and the negatively charged carboxylate O6 atom. Notably, no significant interactions *between* the chains are observed in the presence of Na^+ ions.

When the simulation of two poly-M sequences with Ca^{2+} ions is carried out, an association between the two chains is identified, this time with a V-shaped arrangement, Fig. 5. This association involves interchain carboxylate–Ca^{2+}–carboxylate interactions (as seen previously with G-based decamer chains (Stewart et al., 2014). Interestingly, the Ca^{2+} ions may be observed to spread themselves

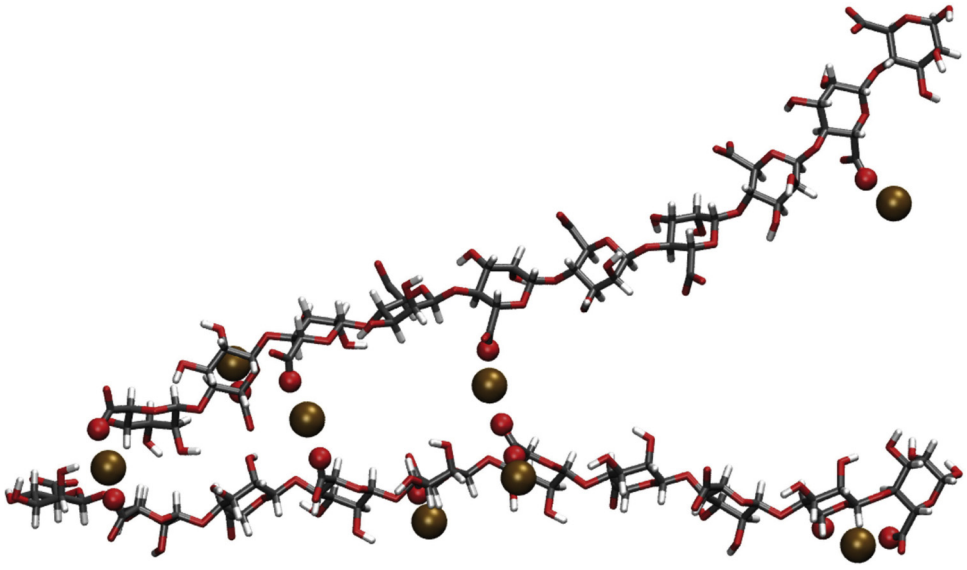

Fig. 5. Molecular dynamics snapshot showing a splayed parallel association of two poly-M chains with Ca^{2+} ions interspersed at equal intervals at the aggregation junction. The ratio is approximately one Ca^{2+} ion for four mannuronate residues. All three interstrand binding modes in this figure are carboxylate–Ca^{2+}–carboxylate bridges. The two chains may be seen to be precluded from 'stitching' by the twisting influence of the intrastrand carboxylate–Ca^{2+}–carboxylate crosslink.

evenly along the chains—occurring at every two residues. However, by the end of this simulation only three Ca^{2+} ions are involved in the consolidated chain association. The binding modes in this case are all identical interstrand carboxylate–Ca^{2+}–carboxylate bridges. It is observed that, approximately 0.1 ns before the end of the simulation, the non-interacting ends of the chains (the ends on the right of Fig. 5) come within 8 Å of each other. The failure of these ends to coalesce in this system can be attributed to the presence of an *intrachain* Ca^{2+}–carboxylate bridge (as characterized in Fig. 3 and discussed previously) that rotates a residue by 180° about the O1 atom resulting in the displacement of a carboxylate moiety that would be needed to complete the junction zone. This is an example of how an *intrastrand* carboxylate–Ca^{2+}–carboxylate bridge can influence the aggregation of strands *via* an *interstrand* bridge, *vide supra*, and could provide an explanation, at the molecular level, for the appearance of ballooning and strand splaying effects that we observe in AFM images of Ca^{2+} alginate gels (Decho, 1999). Intermolecular hydrogen bonding does not appear to have as much influence over chain aggregation with respect to poly-M interactions compared to poly-G interactions as reported previously (Stewart et al., 2014).

4.3. 3× *Poly-M*

When a third mannuronate chain is added and simulated, interchain interactions are observed at two sites, between two of the poly-M chains; these interactions were identified as interchain carboxyate-Ca^{2+} bridging moieties, Fig. 6. The third chain is not observed to interact with the other two chains in this simulation. The orientation of these two interacting chains, however, differs from the 2× poly-M simulations discussed previously, as the chains are not approaching a uniform, parallel alignment. Rather, these two chains are at an angle of ~48° by the end of the simulation. The two interchain binding sites are still separated by a residue, as is discussed in the 2× poly-M system.

This simulation also contains an aspect seen in all of the poly-M simulations that were carried out, namely the rotation around the O1 atom of one of the M residues to form an intrachain carboxylate–Ca^{2+}–carboxylate crosslink. Notably, this motif appears at three sites along these chains, yet only one of these sites resulted in a bend in the mannuronate chain, *vide supra*. However, one of these observed interactions is at an end residue; therefore, whether or not a bend would occur in the extended polymer is unclear. The third site results in only a twist of the chain, rather than a bend. That the same bonding interaction has different effects on the secondary structure of the chain suggests that the specific geometrical outcomes of such modes are influenced by neighbouring structural motifs.

4.4. 1× *Poly-GM*

The simulation of a single poly-GM decamer chain shows that the dominant type of interaction with both Na^{+} and Ca^{2+} ions is *via* carboxylate groups. No unique 'egg-box'-type binding site is identified. This is consistent with conclusions made previously that there is no well-defined binding site for poly-GM sequences (Grant et al., 1973). An intrachain carboxylate–Ca^{2+}–carboxylate bridging interaction, involving adjacent residues and analogous to that identified in the previous poly-M simulations, *i.e.* Fig. 3a, is also present in this simulation. This intrachain binding modality results in a *twisting* of the chain rather than the *bend* that was identified in poly-M. This twisting is evident from a measurement of the change in the plane of adjacent M units—ascertained by measuring χ (the dihedral angle between the O5-C3-O″5-C″3 atoms, Fig. 2c), averaged over the last 300 timesteps. At the ends of the chain, where no effect of the intrachain binding was evident, the average absolute dihedral angles are 162.8° ± 26.4° and 159.4° ± 28.4° (errors equal to two standard deviations). For the dihedral angle measured across the Ca^{2+} binding site, this is reduced to an absolute dihedral angle of 99.3° ± 28.8°, which is a significant difference in planarity. The other interior dihedral angle was measured at 135.7° ± 40° (Fig. S2.)

4.5. 2× *Poly-GM*

When the simulation is carried out with two chains in a Ca^{2+} aqueous environment, a V-shaped motif is observed, Fig. 7. As in previous examples, the interchain interaction is mediated *via* carboxylate–Ca^{2+}–carboxylate bridging. Such interactions are similar to those previously reported for poly-G (Plazinski, 2011) and poly-GM (Donati et al., 2005) chains and are likely to be involved in alginate gelling (Dentini et al., 2007). In this case, the angle between the two chains is ~60°, which is a slightly wider angle than

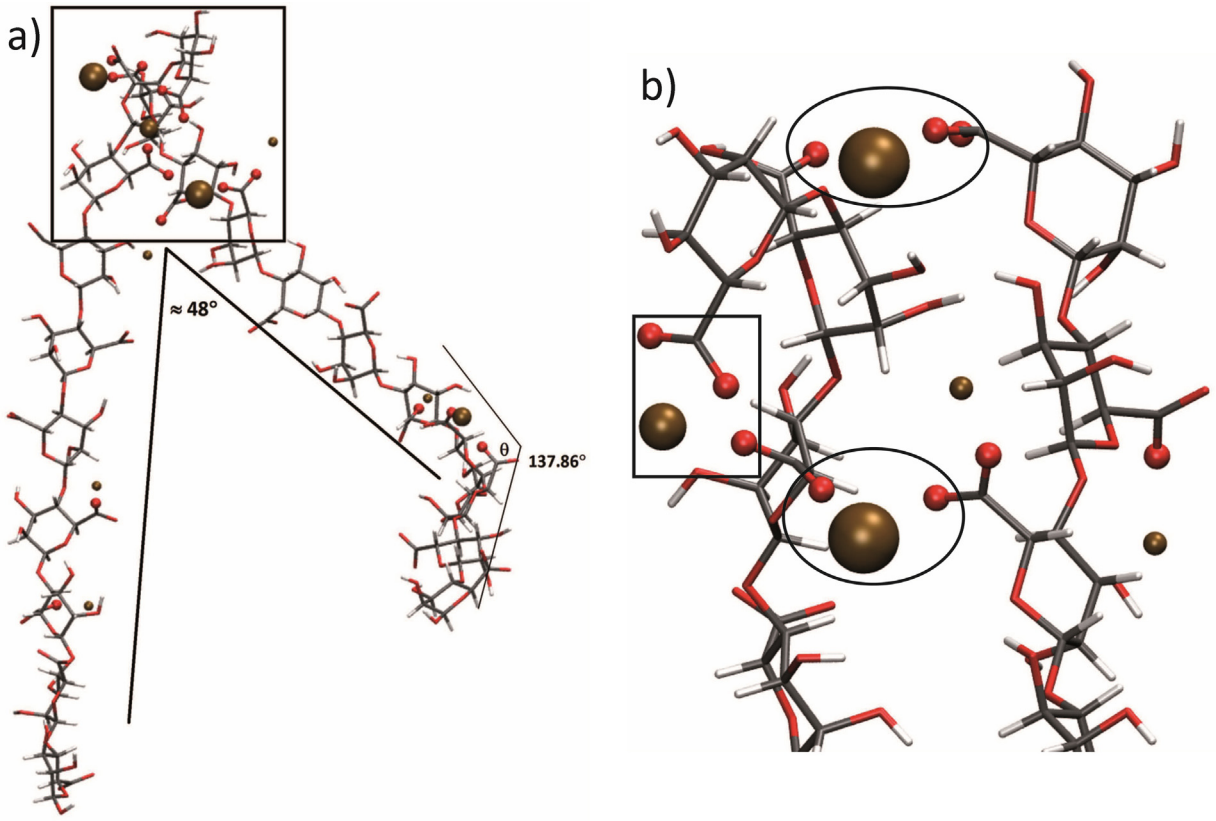

Fig. 6. Molecular dynamics snapshot at the end of the 3× poly-M simulation in the presence of Ca^{2+} (brown spheres) showing (a) the two interacting chains, including the angle between the chains, as well as the bend angle in one of the chains due to an intrachain carboxylate–Ca^{2+} bridging interaction, and (b) a close-up of the interchain interaction site, rotated clockwise 90° from the orientation in (a), showing the interchain (circled) and intrachain (boxed) interactions. Other single carboxylate–Ca^{2+} only interactions are indicated by the reduced-size brown spheres.

was observed for the poly-M simulations, and certainly somewhat removed from the parallel or perpendicular interactions observed for poly-G. Whether this angle is intrinsic, or is an 'end effect' due to the short chain length is difficult to ascertain. However, during the assembly process, such intrinsic (albeit transitory) motifs may be captured and locked into an evolving 3-D network.

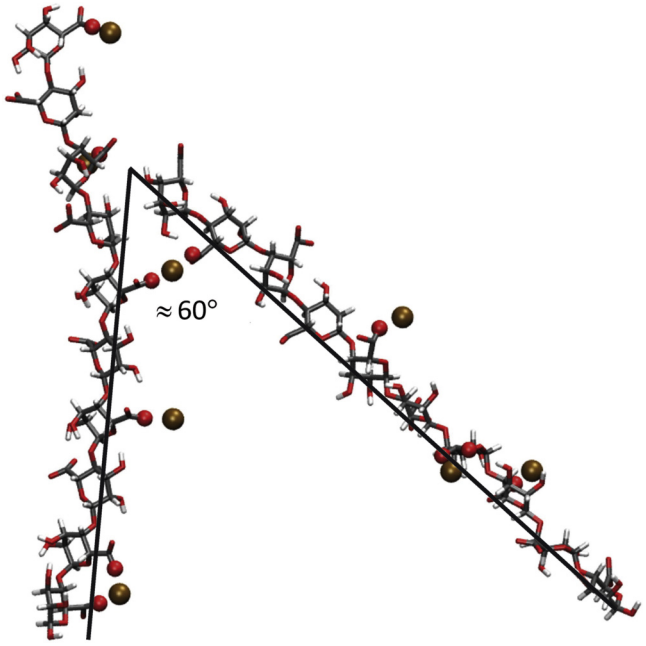

Fig. 7. Aggregation of two GM chains mediated by a Ca^{2+} ion. In this case, there is no defined binding pocket; instead, the junction zone is *via* a single inter-strand carboxylate–Ca^{2+}–carboxylate bridge.

All other occurrences of Ca^{2+} ions interacting with the GM sequence is *via* single carboxylate groups only, except for one instance of an intrachain carboxylate–Ca^{2+}–carboxylate complex, which occurs in a terminal pairing on one chain. Whilst Na^{+} does not show as strong a preference for the carboxylate groups as Ca^{2+}, the radial distribution function (data not shown) showed that the O2 and O3 atoms are also interacting slightly. However, an analysis of the trajectory of this simulation shows that these interactions are occurring independently, rather than being a part of a multi-atom binding site. Due to this binding occurring on the periphery of the chain, in conjunction with the short timeframe of these interactions, there is no discernible effect on the conformation of the chain as a result of Na^{+} binding.

4.6. 3× Poly-GM

The final simulation in this series, involving three alternating GM decamers with Ca^{2+} ions in an aqueous environment, also displays chain aggregation, Fig. S3. This simulation displays a similar binding mode between two of the chains as is seen in the previous two-chain example; as a direct carboxyl–Ca^{2+}–carboxyl complex, with an interchain angle of ∼42°. The third chain lines up parallel with one of the aggregated chains; however, by the end of this simulation there is no direct evidence of interaction, other than the fact that the two chains are in close proximity. There is evidence during the simulation for a second carboxylate bridging interaction (at approximately 0.65 ns of simulation time) although this interaction is eliminated by the end of the simulation.

Table 1
A summary of the main findings of this and the previous study, indicating the most common binding site for the ions present in each simulation, for all possible alginate sequences.

Alginate chains	Ions present	Interactions		
		Carboxylate-ion (non-bridging)	Carboxylate-ion bridge	Binding 'pockets'
1× Poly-G	Ca^{2+}	Yes	Not observed	'Egg-box'-like (Fig. 2a)[a]
2× Poly-G	Ca^{2+}	Yes	Interchain (Fig. 5)[a]	'Shifted egg-box'-like (Fig. 5)[a]
3× Poly-G	Ca^{2+}	Yes	Inter and intrachain (Fig. 7)[a]	Not observed
1× Poly-G	Na^{+}	Yes	Not	Sodium 'egg-box'
2× Poly-G	Na^{+}		observed	(Fig. 2b)[a]
1× Poly-M	Ca^{2+}	Yes	Intrachain (Fig. 3)	Not observed
2× Poly-M	Ca^{2+}	Yes	Inter and Intrachain	Not
3× Poly-M	Ca^{2+}		(Fig. 5)	observed
1× Poly-M	Na^{+}	Yes	Not	'Flattened egg-box'
2× Poly-M	Na^{+}		observed	(Fig. 4)
1× Poly-GM	Ca^{2+}	Yes	Intrachain (Fig. 3)	Not observed
2× Poly-GM	Ca^{2+}	Yes	Intra and Interchain (Fig. 3 and Fig. S3)	Not observed
3× Poly-GM	Ca^{2+}	Yes	Interchain (Fig. S3)	Not observed
1× Poly-GM	Na^{+}	Yes	Not	Not
2× Poly-GM	Na^{+}		observed	observed

[a]Figure references are from previous study (Stewart et al., 2014).

In summary, our results suggest a role for the O2 and O3 atoms in stabilizing sequences of this type, especially with respect to Na^{+} ions. Multi-chain simulations of poly-GM in the presence of aqueous Ca^{2+} results in aggregates that appear to be "more weakly" aligned structures, rather than the more consolidated parallel aggregates that were revealed for poly-G and poly-M. This is consistent with the observation that poly-GM gels are more flexible than poly-G gels (Dentini et al., 2007).

5. Conclusions

In order to probe the effect of sequence on the metal-mediated assembly of alginates gels, MD simulations have resulted in the characterisation of a variety of intrinsic binding modes for the interaction of sodium and calcium ions with poly-M and poly-GM alginate decamers in an aqueous environment at neutral to alkaline pH. These have been compared with previous analogous results reported for the interaction of these ions with poly-G (Stewart et al., 2014). Depending upon the specific sequence, there were found to be clear differences in metal ion binding mode preferences. This is also reflected in differences in how different chains initiate aggregation and, as in the previous poly-G study, a range of potential motifs have been uncovered that are consistent with previous molecular-scale imaging of an alginate gel network (Decho, 1999). The binding modes observed for all three sequences are summarized in Table 1. Binding modes based on the standard 'egg-box' pocket appear to be more favoured for GG sequences (GG ≫ MM > GM). Not surprisingly, direct interactions of both ions with single carboxylate moieties are common. The formation of inter and intrachain carboxylate–Ca^{2+}–carboxylate bridging is also observed for all sequences. Such interactions are not observed for Na^{+}. An important finding is that the intrastrand carboxylate–Ca^{2+}–carboxylate binding mode can result in significant chain distortions (such as twists and bends)—the precise nature of which appears to depend on the immediate binding site environment. Notably, this *intrastrand* effect has important *interstrand* consequences. Thus such distortions can impact on how the chains subsequently aggregate—as demonstrated in the 2× poly-M simulation, where this mode can be seen to preclude the "stitching together" of one section of two parallel poly-M chains, *vide supra*.

The fact that poly-M decamers aggregate in the presence of Ca^{2+}, utilizing a mechanism similar to that found with poly-G decamers; namely *via* tight binding carboxylate bridging interactions, suggests that poly-M regions may play a role in network assembly, especially considering that the chains are at angles of ∼45°. This may support the notion that the poly-M sequence is involved in secondary crosslinking interactions. Indeed, in previous work on the use of calcium-alginate as a membrane construction material (Kashima and Imai, 2011), it is observed, *via* SEM imaging, that alginates relatively low in poly-G regions are still capable of forming a smooth surface (*i.e.* high degree of calcium-induced cross-linking)—albeit at higher concentrations of Ca^{2+} than those required for alginates containing a higher proportion of poly-G regions.

For all sequences (including the previously reported poly-G), different chain aggregation patterns (motifs) are evident that range from parallel to perpendicular and all such associations are mediated by calcium ions only. Unique arrangements from the present study include a parallel association between two poly-M decamers that is 'splayed' at one end due to the influence of an intra-chain carboxylate–Ca^{2+}–carboxylate bridge, as described previously. In the 3× poly-M simulation, two decamers are arranged at an angle of ∼48° secured by a junction zone involving three calcium ions. Other angular arrangements of ∼60° are observed for poly-GM secured by junction zones involving two and three calcium ions. Further work is underway to extend these studies to the heterogeneous poly-G/poly-M, poly-G/poly-GM and poly-M/poly-GM calcium-mediated decamer interactions.

Acknowledgement

The authors would like to acknowledge Victoria University for providing a Postdoctoral Fellowship to MBS and thank Dr. Michael Kuiper and the Victorian Partnership for Advanced Computing (VPAC) for technical assistance and computing resources which contributed to this work.

Appendix A. Supplementary data

Supplementary material related to this article can be found, in the online version, at http://dx.doi.org/10.1016/j.carbpol.2014.06.001.

References

BeMiller, J. N. (2009). One hundred years of commercial food carbohydrates in the United States. *Journal of Agricultural and Food Chemistry*, *57*(18), 8125–8129.
Braccini, I., Grasso, R. P., & Pérez, S. (1999). Conformational and configurational features of acidic polysaccharides and their interactions with calcium ions: A molecular modeling investigation. *Carbohydrate Research*, *317*, 119–130.
Braccini, I., & Pérez, S. (2001). Molecular basis of Ca^{2+}-induced gelation in alginates and pectins: The egg-box model revisited. *Biomacromolecules*, *2*, 1089–1096.

Davis, T. A., Volesky, B., & Mucci, A. (2003). A review fo the biochemistry of heavy metal biosorption by brown algae. *Water Research*, *37*(18), 4311–4330.
Decho, A. W. (1999). Imaging an alginate polymer gel matrix using atomic force microscopy. *Carbohydrate Research*, *315*, 330.
Dentini, M., Rinaldi, G., Barbetta, A., Risica, D., Anselmi, C., & Skjåk-Bræk, G. (2007). Ionic gel fornation of a (pseudo)alginate characterised by an alternating MG sequence produced by epimerising mannuronan with AlgE4. *Carbohydrate Polymers*, *67*(4), 465–473.
DeRamos, C. M., Irwin, A. E., Nauss, J. L., & Stout, B. E. (1997). ^{13}C NMR and molecular modeling studies of alginic acid binding with alkaline earth and lanthanide metal ions. *Inorganica Chimica Acta*, *256*, 69–75.
Donati, I., Holtan, S., Mørch, Y. A., Borgogna, M., Dentini, M., & Skjåk-Bræk, G. (2005). New hypothesis on the role of alternating sequences in calium-alginate gels. *Biomacromolecules*, *6*, 1031–1040.
Donati, I., & Paoletti, S. (2009). Material properties of alginates. In B. H. A. Rehm (Ed.), *Alginates: Biology and applications*. Berlin Heidelberg: Springer.
Dudev, T., & Lim, C. (2004). Monodentate versus bidentate carboxylate binding in magnesium and calicum proteins: What are the basic principles? *Journal of Physical Chemistry B*, *108*, 4546–4557.
Einspahr, H., & Bugg, C. E. (1981). The geometry of calcium–carboxylate interactions in crystalline complexes. *Acta Crystallographica*, *B37*, 1044–1052.
Ertesvåg, H., Valla, S., & Skjåk-Bræk, G. (1996). Genetics and biosynthesis of alginates. *Carbohydrates in Europe*, *14*, 14–18.
Gorin, P. A. J., & Spencer, J. F. T. (1966). Exocellular alginic acid from *Azotobacter vinelandii*. *Canadian Journal of Chemistry*, *44*, 993–998.
Goven, J. R., Fyfe, J. A., & Jarman, T. R. (1981). Isolation of alginate-producing mutants of *Pseudomonas fluorescens*, *Pseudomonas putida* and *Psuedomonas mendocina*. *Journal of General Microbiology*, *125*, 217–220.
Grant, G. T., Morris, E. R., Rees, D. A., Smith, P. J. C., & Thom, D. (1973). Biological interactions between polysaccharides and divalent cations: The egg-box model. *FEBS Letters*, *32*(1), 195–198.
Grasdalen, H. (1983). High-field, ^{1}H-N.M.R. spectroscopy of alginate: Sequential structure and linkage conformations. *Carbohydrate Research*, *118*, 255–260.
Grasdalen, H., Larsen, B., & Smidsrød, O. (1977). ^{13}C-NMR studies of alginate. *Carbohydrate Research*, *56*, C11–C15.
Grasdalen, H., Larsen, B., & Smidsrød, O. (1979). A p.m.r study of the composition and sequence of uronate residues in alginates. *Carbohydrate Research*, *68*, 23–31.
Grasdalen, H., Larsen, B., & Smidsrød, O. (1981). ^{13}C-NMR studies of monomeric composition and sequence in alginate. *Carbohydrate Research*, *89*, 179–191.
Haug, A., Larsen, B., & Smidsrød, O. (1966). A study on the constitution of alginic acid by partial hydrolysis. *Acta Chemica Scandinavica*, *20*, 183–190.
Haug, A., Larsen, B., & Smidsrød, O. (1967). Studies on the sequence of uronic acid residues in alginic acid. *Acta Chemica Scandinavica*, *21*, 691–704.
Haug, A., & Smidsrød, O. (1965). Fractionation of alginate by precipitation with calcium and magnesium ions. *Acta Chemica Scandinavica*, *19*, 1221–1226.
Holtan, S., Bruheim, P., & Skjåk-Bræk, G. (2006). Mode fo action and subsite studies of the guluronan block-forming mannuronan C-5 epimerases AlgE1 and Alg E6. *Biochemical Journal*, *395*, 319–329.
Humphrey, W., Dalke, A., & Schulten, K. (1996). VMD—visual molecular dynamics. *Journal of Molecular Graphics*, *14*, 33–38.
Katz, A. K., Glusker, J. P., Beebe, S. A., & Bock, C. W. (1996). Calcium ion coordination: A comparison with that of beryllium, magnesium and zinc. *Journal of the American Chemical Society*, *118*, 5752–5763.
Kashima, K., & Imai, M. (2011). Dominant impact of the α-L-guluronic acid chain on regulation of the mass transfer character of calcium alginate membranes. *Desalination and Water Treatment*, *34*, 257–265.
Langer, R., & Tirrell, D. A. (2004). Designing materials for biology and medicine. *Nature*, *428*, 487–492.
Li, L., Fang, Y., Vreeker, R., & Appelqvist, I. (2007). Reexamining the egg-box model in calcium—Alginate gels with X-ray diffraction. *Biomacromolecules*, *8*, 464–468.
MacKerell, A. D., Bashford, D., Bellott, M., Dunbrack, R. L., Evanseck, J. D., Field, M. J., & Karplus, M. (1998). All-atom empirical potential for molecular modeling and dynamics studies of proteins. *The Journal of Physical Chemistry B*, *102*(18), 3586–3616. http://dx.doi.org/10.1021/jp973084f
Phillips, J. C., Braun, R., Wang, W., Gumbart, J., Tajkhorshid, E., Villa, E., & Schulten, K. (2005). Scalable molecular dynamics with NAMD. *Journal of Computational Chemistry*, *26*, 1781–1802.
Plazinski, W. (2011). Molecular basis of calcium binding by polyguluronate chains. Revising the egg-box model. *Journal of Computational Chemistry*, *32*(14), 2988–2995.
Skjåk-Bræk, G., Grasdalen, H., & Larsen, B. (1986). Monomer sequence and acetylation pattern in some bacterial alginates. *Carbohydrate Research*, *154*, 239–250.
Stewart, M. B., Gray, S. R., Vasiljevic, T., & Orbell, J. D. (2014). Exploring the molecular basis for the metal-mediated assembly of alginate gels. *Carbohydrate Polymers*, *102*, 246–253.